JACS
JOURNAL OF THE AMERICAN CHEMICAL SOCIETY

COMMUNICATION

pubs.acs.org/JACS

Gene Silencing by siRNA Microhydrogels via Polymeric Nanoscale Condensation

Cheol Am Hong,[†] Soo Hyeon Lee,[†] Jee Seon Kim,[†] Ji Won Park,[†] Ki Hyun Bae,[†] Hyejung Mok,[⊥] Tae Gwan Park,[†,§] and Haeshin Lee[‡,§]

[†]Department of Biological Sciences, [‡]Molecular-level Interface Research Center, Department of Chemistry, and [§]The Graduate School of Nanoscience & Technology (WCU), Korea Advanced Institute of Science and Technology (KAIST), Daejeon 305-701, South Korea

[⊥]BioNanotechnology Research Center, Korea Research Institute of Bioscience and Biotechnology (KRIBB), 111 Science Road, Daejeon 305-806, South Korea

Supporting Information

ABSTRACT: The first attempt to prepare biologically active siRNA-based microhydrogels is reported. The self-assembled microhydrogels were fabricated using sense/antisense complementary hybridization between single-stranded linear and Y-shaped trimeric siRNAs. The siRNA microhydrogels were condensed using a popular cationic polymer such as LPEI to form compact, stable siRNA/polymeric nanoparticles that exhibited superb cellular uptake efficiency and gene silencing activity.

DNA has been exploited as an excellent molecular building block for fabricating a wide range of two- and three-dimensional nanostructures with different sizes, shapes, and patterns due to its highly specific complementary base pairing.[1,2] A variety of predictable nanoarchitectures including grids, cubes, and polyhedra have been readily constructed in a precisely controlled manner by rationally designed DNA strands.[3] DNA-based dendrimers and hydrogels have also been synthesized using Y-shaped, trimeric DNA molecules that serve as cross-linkers for self-assembling two or more designed sequences via ligase-mediated reactions.[4] Although the self-assembled DNA nanostructures and hydrogels exhibit a variety of structures with well-defined geometry, they generally do not show any biological activity at a molecular and cellular level. Small interfering RNA (siRNA), which is composed of double-stranded (ds) RNA molecules with approximately 21−27 base pairs, has recently emerged as a powerful tool for silencing target genes.[5,6] Compared to single-stranded (ss) antisense oligonucleotides, siRNA has shown enhanced gene silencing with high specificity at low doses.[7,8]

In this study, siRNA microhydrogels with gene silencing activity were prepared by hybridization between ss sense and antisense siRNAs containing Y-shaped siRNA branches as hinge-like cross-linkers without enzyme-catalyzed ligation. As shown in Figure 1, ss sense/antisense green fluorescent protein (GFP) siRNA with a thiol group at the 3′-end was reacted with the trimeric cross-linker tri-[2-maleimidoethyl]-amine (TMEA) to prepare Y-shaped siRNAs and with a dimeric cross-linker 1,8-bis(maleimidodiethylene) glycol [BM(PEG)$_2$] for dimeric siRNAs. Hybridization reactions were performed by mixing an equal amount of the sense and antisense siRNA solutions (phosphate-buffered saline (PBS), pH 7.4) under mild agitation. The resulting products contained Y-shaped trimeric, dimeric, and monomeric siRNAs and were separated using 15% polyacrylamide gel electrophoresis (PAGE) (Supporting Information, Figure S1a). The ss antisense siRNA species were composed of 16% trimers, 63% dimers, and 19% monomers, which were determined by gel permeation chromatography (GPC) analysis (Supporting Information Figure S1b). The ss sense siRNA species, which were synthesized in the same manner as the ss antisense siRNA species, were composed of 13% trimers, 74% dimers, and 12% monomers (data not shown). The yield to generate the linear, dimeric siRNA that was linked with BM(PEG)$_2$ was over 80% for sense/antisense siRNAs, which were determined by 15% PAGE (Supporting Information Figure S2a) and GPC analysis (Supporting Information Figures S2b,c).

Three types of annealing reaction products were produced: (i) multimeric siRNAs (M-siRNA) by mixing the dimeric sense/antisense siRNAs, (ii) branched siRNAs by combining the dimeric, linear sense and Y-shaped antisense siRNAs (DY-siRNA), and (iii) branched siRNAs by the Y-shaped sense/antisense siRNAs (YY-siRNA) (Figure 1). The method for producing M-siRNA was based on our previous report.[9] Self-assembled M-siRNA, DY-siRNA, and YY-siRNA were analyzed by 15% PAGE as shown in Figure 2a. M-siRNA displayed multiple ladder-like bands in the gel, indicating the formation of multimerized siRNAs as previously reported.[9] On the other hand, DY-siRNA and YY-siRNA remained in the sample loading zone, showing intense bands unlike the ladder-like multimeric M-siRNA species, suggesting hyper-cross-linked siRNA structures. YY-siRNA exhibited stronger band intensity in the loading zone than DY-siRNA, implying that YY-siRNA displayed a greater extent of cross-linking than that of DY-siRNA. The PAGE results reveal that hyper-cross-linked siRNA networks may be readily produced by hybridization when Y-shaped siRNA trimers are involved.

Atomic force microscopy (AFM) and confocal microscopy were used to examine the morphology and size of DY-siRNA and YY-siRNA in dry and wet states. As shown in Figure 2d,e, the dehydrated DY-siRNA and YY-siRNA showed well-dispersed spherical morphology, with an average size of 3.7 ± 1.9 μm and 2.0 ± 0.8 μm, respectively. In contrast, monomeric siRNA and M-siRNA exhibited markedly different nanometer-scale dots that were consistent with our previous study[10] (Figure 2b,c). The siRNA concentrations of the solutions were identical (0.7 μM). DY-siRNA exhibited more porous structures compared to YY-siRNA. Using section analysis of the AFM images, DY-siRNA and YY-siRNA

Received: June 30, 2011
Published: August 10, 2011

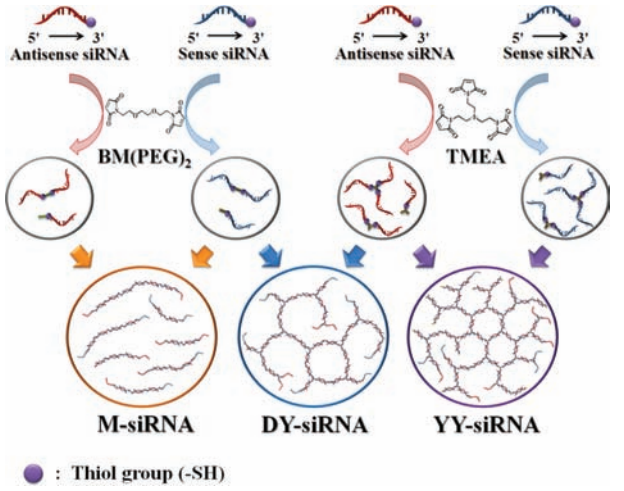

Figure 1. Synthetic scheme for the preparation of multimeric siRNA (M-siRNA) and siRNA microhydrogels with larger pores (DY-siRNA) and with smaller pores (YY-siRNA).

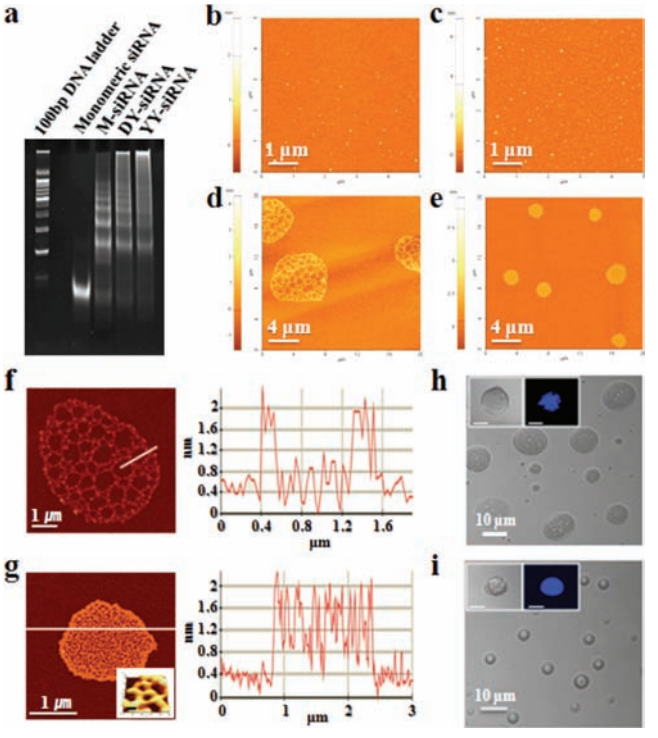

Figure 2. Physicochemical characterization of siRNA microhydrogels. (a) PAGE analysis of monomeric siRNA, M-siRNA, DY-siRNA, and YY-siRNA. AFM images of monomeric siRNA (b), M-siRNA (c), DY-siRNA (d), and YY-siRNA (e). Scale bar = 1 μm (b,c) and 4 μm (d,e). High-resolution AFM images of DY-siRNA (f) and YY-siRNA (g) and their section analysis. Scale bar = 1 μm. The inset in the panel g is a high-magnification 3-D AFM image of YY-siRNA. Confocal microscopy images of DY-siRNA (h) and YY-siRNA (i) in aqueous solution (Inset: DAPI-stained DY- and YY-siRNA). Scale bar = 10 μm.

showed pore sizes of 484 ± 28 nm and 59 ± 13 nm, respectively (Figure 2f,g). Many nanoscale pores appeared to be enclosed by a network of the cross-linked siRNAs. Multiple Y-branched junctions in the magnified AFM images were observed, suggesting that DY- and YY-siRNA formed three-dimensional networks by complementary siRNA sequences. DY-siRNA had a larger pore dimension compared to YY-siRNA because ss sense dimeric siRNA significantly extended the mesh length between the two adjacent Y junctions compared to the length that was formed using Y-shaped siRNA alone. Thus, the difference in the mesh length between two junctions was controlled by linear and Y-shaped siRNA species and mediated the overall sizes of DY-siRNA and YY-siRNA microstructures, which are shown in Figure 2d,e. The thickness of the ds siRNA backbone, which was observed in the AFM images, was far greater than that of ds siRNA (approximately 2 nm). This difference was probably caused by a 10 nm AFM tip in a noncontact mode to scan the cross-linked siRNA objects on the surface.[11,12] The height of the ds siRNA backbone in the siRNA microstructure was approximately 2 nm (Figure 2f,g), which was consistent with the actual thickness of ds siRNA. Confocal microscopy images demonstrated that the DY-siRNA and YY-siRNA structures exhibited spherical, swollen microhydrogels in an aqueous solution. The average sizes of DY-siRNA and YY-siRNA were 11.4 ± 4.7 μm and 7.8 ± 2.3 μm, respectively, which were slightly larger than those indicated by the AFM data due to the hydration of the siRNA chain network.[13] The intense blue-colored siRNA microhydrogels were observed after staining with 4′,6-diamidino-2-phenylindole (DAPI), which specifically intercalates into ds nucleic acids. These results reveal that siRNA microhydrogels are composed of 100% siRNA molecules. The YY-siRNA displayed more intense DAPI staining than DY-siRNA due to the formation of compact network structures. The DY- and YY-siRNA microhydrogels were spontaneously produced in an aqueous solution under mild stirring conditions by the self-assembly process of two complementary sequences of ss sense/antisense siRNAs. During the self-assembly, monomeric siRNA served as a chain terminator, dimeric siRNA extended the chain length, and Y-shaped trimeric siRNA functioned as a cross-linker in the siRNA network structure. These structures did not show any evidence of the formation of a large siRNA hydrogel mass in the aqueous solution. These results indicate that the self-assembly process to form spherical siRNA microgels is probably controlled by the concentration of two complementary siRNA species, agitation speed, and hybridization kinetics.

The YY- and DY-siRNA microhydrogels with hollow and porous internal structures due to intramolecular charge repulsion exhibited 95.7-fold and 78.8-fold size transition by the complexation with a cationic polymer, linear polyethylenimine (LPEI: M_w 2500). As shown in Figure 3c,d, the highly porous siRNA microhydrogels collapsed to form polyelectrolyte complexes that were approximately 100 nm in size. The nanogel complexes, which were formed by a nitrogen/phosphate (N/P) ratio of 60, were 215 ± 125 nm for M-siRNA, 119 ± 44 nm for DY-siRNA, and 99 ± 42 nm for YY-siRNA. Monomeric siRNA/LPEI complexes exhibited heterogeneous, micrometer-sized aggregates (Figure 3a). In contrast, DY-siRNA and YY-siRNA produced compact nanocomplexes upon interactions with LPEI (<120 nm) compared to the large size of nanoparticles that were formed by M-siRNA/LPEI complexes (>200 nm) (Figure 3b−d). The formation of stable, compact polyelectrolyte complexes (DY- and YY-siRNA/LPEI) with LPEI, which is a weakly charged cationic carrier, indicated that microhydrogels have enhanced charge densities compared to that of M-siRNAs.[14] Also, the DY-and YY-siRNA/LPEI complexes showed improved stability in a 50% (v/v) serum solution (Supporting Information Figure S3). In general, monomeric siRNA may not form any stable nanocomplexes with conventional cationic polymers due to the low charge density of siRNA. This unique electrostatic property of siRNAs has triggered extensive studies to develop new

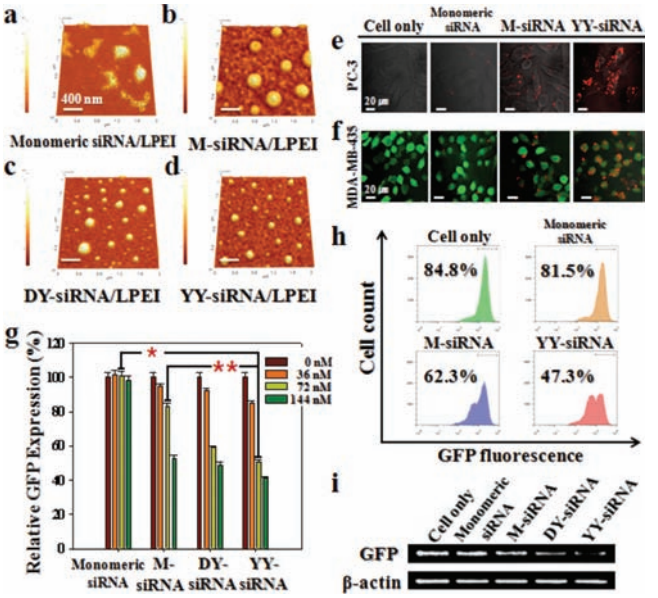

Figure 3. Gene silencing effects of siRNA microhydrogels for breast cancer cells. AFM images of monomeric siRNA/LPEI (a), M-siRNA/LPEI (b), DY-siRNA/LPEI (c), and YY-siRNA/LPEI (d) complexes. Scale bar = 400 nm. Confocal microscopy images of intracellular uptake of siRNA complexes formulated with Cy5-labeled LPEI for PC-3 (e) and GFP overexpressed MDA-MB-435 cells (f). Scale bar = 20 μm. (g) Dose-dependent GFP gene silencing effect mediated by various siRNA/LPEI complexes for GFP overexpressed MDA-MB-435 cells. * and ** $p < 0.05$. (h) FACS analysis of GFP overexpressed MDA-MB-435 cells transfected with various siRNA/LPEI complexes. The percentage shows the number of cells sorted within a prefixed gate region. (i) Semiquantitative RT-PCR analysis for intracellular GFP mRNA levels after transfection with various siRNA/LPEI complexes. Human β-actin was used as a control.

polymeric carriers that efficiently deliver siRNA therapeutics.[15] In place of carriers, engineered siRNA structures with high charge densities such as DY- and YY-siRNA microhydrogels, which are described herein, may serve as an alternative new strategy for highly efficient intracellular delivery. An advantage of this new formulation is that the nanoparticles do not exhibit any cytotoxicity (Supporting Information Figure S4).

Extents of cellular uptake of monomeric siRNA, M-, DY-, and YY-siRNA complexes formulated with Cy5-labeled LPEI were visualized using confocal microscopy. YY-siRNA/LPEI-Cy5 complexes were more efficiently taken up by PC-3 (Figure 3e) and MDA-MB-435 (Figure 3f) cells than monomeric and M-siRNA/LPEI-Cy5 complexes (Figure 3e,f; second and third panels). The cells treated with YY-siRNA/LPEI-Cy5 complexes showed more scattered, multiple bright red fluorescent dots in the cytoplasm than the cells treated by M-siRNA/LPEI-Cy5 complexes (Figure 3e,f; fourth panels). It has been known that stable and dense nanoparticles with a size less than 150 nm are efficiently internalized into cells via an endocytic pathway.[16] The dense and compact YY-siRNA/LPEI nanocomplexes were efficiently endocytosed compared to M-siRNA/LPEI complexes (Figure 3e,f; third and fourth panels). Likewise, DY-siRNA/LPEI-Cy5 complexes also demonstrated cellular uptake that was comparable to that by YY-siRNA/LPEI-Cy5 complexes (data not shown).

The GFP gene silencing efficiency of the monomeric siRNA, M-, DY-, and YY-siRNA complexes that were formulated with LPEI were evaluated by transfecting them into GFP-overexpressing MDA-MB-435 cells (Figure 3g). The extent of gene inhibition was quantitatively analyzed by measuring the intracellular GFP fluorescence intensity after transfection. DY- and YY-siRNA complexes significantly inhibited GFP expression by 58.9 $\pm$ 1.1% and 50.8 $\pm$ 1.4%, respectively (light green bars, 72 nM). This finding indicated an enhanced gene silencing effect compared to that of M-siRNAs complexes (83.1 $\pm$ 1.6%) at siRNA concentration of 72 nM. In contrast, monomeric siRNA complexes did not show any noticeable gene silencing activities, even when an increased amount of siRNA was used (up to 144 nM). All M-, DY-, and YY-siRNA complexes demonstrated dose-dependent GFP gene-silencing behaviors. However, DY- and YY-siRNA complexes showed more efficient gene silencing than M-siRNA complexes overall. GFP gene silencing was also examined using fluorescence-activated cell sorter (FACS) analysis (Figure 3h). Using a siRNA concentration of 72 nM, M- and YY-siRNA/LPEI complexes showed significant fluorescence intensity shifts from 84.8% to 62.3% for M-siRNA/LPEI and from 84.8% to 47.2% for YY-siRNA/LPEI. The FACS data were consistent with the GFP silencing levels, which were determined by the intracellular fluorescence intensity (Figure 3g,h; 72 nM). Semiquantitative reverse-transcription polymerase chain reaction (RT-PCR) analysis was performed to determine the GFP mRNA levels after transfection. Using a siRNA concentration of 72 nM, the relative band intensities of GFP mRNA in the cells that were treated with monomeric siRNA, M-, DY-, and YY-siRNA were 87.7%, 70.5%, 43.5%, and 27.9%, respectively, which were measured using *Image J* software (Figure 3i). These results strongly suggest that the gene silencing effects of DY- and YY-siRNA were mediated by degradation of a target GFP mRNA.

We demonstrated that the new branched siRNA structures of DY- and YY-siRNA formed 3D microhydrogels via complementary base pair self-assembly with 21 bp siRNA. There were no acid-labile or reducible cleavable linkages in the microhydrogels that could be disintegrated by acidic pH environments and/or reductive glutathione species in the cytoplasm. To silence a target gene, the siRNA microhydrogels must be cleaved by intracellular RNA enzymes to produce smaller fragments that bind to RNA-induced silencing complexes (RISC) to mediate RNAi mechanisms. An endoribonuclease, Dicer, recognizes even artificial, unusual siRNA molecules that form long and linear ds RNAs and subsequently cleaves random positions of the ds RNAs.[17] Therefore, we hypothesized that the novel 3-D microhydrogels may function as substrates for Dicer in a manner similar to that shown for 1-D ds long-chain RNAs. To confirm that the siRNA microhydrogels may act as Dicer substrates to produce short ds siRNA fragments, YY-siRNA was treated with Dicer, and the resulting products were verified by 15% PAGE analysis (data not shown). After Dicer treatments, we observed that YY-siRNA was degraded into random siRNA fragments. This result suggests that intracellular YY-siRNA was initially processed by Dicer to generate random ds siRNA species that participated in RNAi mechanisms to inhibit target gene expression. On the basis of our previous study of cleavable and noncleavable M-siRNAs, the observed gene silencing effect by noncleavable siRNA microhydrogels was probably caused by the post-transcriptional repression and degradation of target mRNA, including microRNA (miRNA)-related RNAi mechanisms.[9]

In conclusion, we demonstrated a novel strategy to prepare biologically active siRNA-based microhydrogels that self-assemble via complementary base pairing. The siRNA-based microhydrogels with substantially increased charge density collapsed to form compact nanosized complexes upon interacting with

the popular cationic carrier LPEI. Furthermore, the complexes exhibited superb cellular uptake and gene silencing activities. Our results suggest that siRNA microhydrogels may be useful as a new class of nucleic acid platform materials for therapeutic applications.

■ ASSOCIATED CONTENT

Supporting Information. Detailed experimental procedures and supporting figures. This material is available free of charge via the Internet at http://pubs.acs.org.

■ AUTHOR INFORMATION

Corresponding Author
haeshin@kaist.ac.kr; tgpark@kaist.ac.kr

■ ACKNOWLEDGMENT

The authors express their sincere condolences to the family on the death of Prof. Tae Gwan Park. This study was supported by the grants from the Ministry of Health and Welfare and National Research Foundation of S. Korea: Nano Therapeutic and Diagnostic Center (2010-0027955), Cancer Control R&D Program (920340), and WCU Program (R31-10071-0), and MIRC (2011-0001319).

■ REFERENCES

(1) (a) Seeman, N. C. *Trends Biochem. Sci.* **2005**, *30*, 119–125. (e) *Nature* **2003**, *421*, 427–431. (b) Rothemund, P. W. K. *Nature* **2006**, *440*, 297–302. (c) Lee, J. B.; Roh, Y. H.; Um, S. H.; Funabashi, H.; Cheng, W.; Cha, J. J.; Kiatwuthinon, P.; Muller, D. A.; Luo, D. *Nat. Nanotechnol.* **2009**, *4*, 430–436. (d) Park, S. H.; Pistol, C.; Ahn, S. J.; Reif, J. H.; Lebeck, A. R.; Dwyer, C.; LaBean, T. H. *Angew. Chem., Int. Ed. Engl.* **2006**, *45*, 735–739.

(2) (a) Felkamp, U.; Niemeyer, C. M. *Angew. Chem., Int. Ed. Engl.* **2006**, *45*, 1856–1876. (b) Winfree, E.; Liu, F. R.; Wenzler, L. A.; Seeman, N. C. *Nature* **1998**, *394*, 539–544.

(3) (a) Chen, J.; Seeman, N. C. *Nature* **1991**, *350*, 631–633. (b) Yan, H.; Park, S. H.; Finkelstein, G.; Reif, J. H.; LaBean, T. H. *Science* **2003**, *301*, 1882–1884. (c) He, Y.; Ye, T.; Su, M.; Zhang, C.; Ribbe, A. E.; Jiang, W.; Mao, C. *Nature* **2008**, *452*, 198–201.

(4) (a) Li, Y.; Tseng, Y. D.; Kwon, S. Y.; d'Espaux, L.; Bunch, J. S.; McEuen, P. L.; Luo, D. *Nat. Mater.* **2004**, *3*, 38–42. (b) Um, S. H.; Lee, J. B.; Park, N.; Kwon, S. Y.; Umbach, C. C.; Luo, D. *Nat. Mater.* **2006**, *5*, 797–801. (c) Cheng, E.; Xing, Y.; Chen, P.; Yang, Y.; Sun, Y.; Zhou, D.; Xu, L.; Fan, Q.; Liu, D. *Angew. Chem., Int. Ed.* **2009**, *48*, 7660–7663.

(5) (a) Moazed1, D. *Nature* **2009**, *457*, 413–420. (b) Dykxhoorn, D. M.; Palliser, D.; Lieberman, J. *Gene Ther.* **2006**, *13*, 541–552. (c) Jackson, A. L.; Linsley, P. S. *Nat. Rev. Drug Discovery* **2010**, *9*, 57–67.

(6) (a) Bhargava, A.; Dallman, M. F.; Pearce, D.; Choi, S. *Brain Res. Proc.* **2004**, *13*, 115–125. (b) Brondani, V.; Zhang, H.; Muller, U.; Filipowicz, W. *Proc. Natl. Acad. Sci. U.S.A.* **2001**, *98*, 14428–14433.

(7) (a) Holen, T.; Amarzguioui, M.; Babaie, E.; Prydz, H. *Nucleic Acids Res.* **2003**, *31*, 2401–2407. (b) Martinez, J.; Patkaniowska, A.; Urlaub, H.; Lührmann, R.; Tuschl, T. *Cell* **2002**, *110*, 563–574.

(8) (a) Xu, Y.; Linde, A.; Larsson, O.; Thormeyer, D.; Elmen, J.; Wahlestedt, C.; Lianga, Z. *Biochem. Biophy. Res. Commun.* **2004**, *316*, 680–687. (b) Elbashir, S. M.; Lendeckel, W.; Tuschl, T. *Genes Dev.* **2001**, *15*, 188–200.

(9) (a) Mok, H.; Lee, S. H.; Park, J. W.; Park, T. G. *Nat. Mater.* **2010**, *9*, 272–278. (b) Lee, S. H.; Mok, H.; Jo, S.; Hong, C. A.; Park, T. G. *Biomaterials* **2011**, *32*, 2359–2368.

(10) (a) Mao, S.; Neu, M.; Germershaus, O.; Merkel, O.; Sitterberg, J.; Bakowsky, U.; Kissel, T. *Bioconjugate Chem.* **2006**, *17*, 1209–1218. (b) Hansma, H. G.; Revenko, I.; Kim, K.; Laney, D. E. *Nucleic Acids Res.* **1996**, *24*, 713–720. (c) Podgornik, R. *Nat. Nanotechnol.* **2006**, *1*, 100–101.

(11) (a) Sedin, D. L.; Rowlen, K. L. *Appl. Surf. Sci.* **2001**, *182*, 40–48. (b) Schmitz, I.; Schreiner, M.; Friedbacher, G.; Grasserbauer, M. *Anal. Chem.* **1997**, *69*, 1012–1018.

(12) (a) Markiewicz, P.; Goh, C. M. *Langmuir* **1994**, *10*, 5–7. (b) Leung, C. W.; Markiewicz, P.; Goh, C. M. *J. Vac. Sci. Technol., B* **1997**, *15*, 181–185. (c) Vesenka, J.; Miller, R.; Henderson, E. *Rev. Sci. Instrum.* **1994**, *7*, 2249–2251. (d) Gondran, C. F. H.; Michelson, D. K. *J. Vac. Sci. Technol.* **2006**, *141*, 1185–1191.

(13) (a) Pal, S. K.; Zhao, L.; Zewail, A. H. *Proc. Natl. Acad. Sci. U.S.A.* **2003**, *100*, 8113–8118. (b) Berman, H. M. *Curr. Opin. Struct. Biol.* **1991**, *273*, 423–427. (c) Schneider, B.; Patel, K.; Berman, H. M. *Biophy. J.* **1998**, *75*, 2422–2434.

(14) (a) Xu, S.; Dong, M.; Liu, X.; Howard, K. A.; Kjems, J.; Besenbacher, F. *Biophys. J.* **2007**, *93*, 952–959. (b) Kim, W. J.; Kim, S. W. *Pharm. Res.* **2008**, *25*, 657–666.

(15) (a) Langer, R.; Anderson, D. G.; et al. *Nat. Biotechnol.* **2008**, *26*, 561–569. (b) Zhang, S.; Zhao, B.; Jiang, H.; Wang, B.; Ma, B. *J. Controlled Release* **2007**, *123*, 1–10.

(16) (a) Grayson, A. C.; Doody, A. M.; Putnam, D. *Pharm. Res.* **2006**, *23*, 1868–1876. (b) Mok, H.; Park, J. W.; Park, T. G. *Bioconjugate Chem.* **2007**, *14*, 1483–1489.

(17) (a) Kim, D.; Behlke, M. A.; Rose, S. D.; Chang, M.; Choi, S.; Rossi, J. J. *Nat. Biotechnol.* **2004**, *23*, 222–226. (b) Chang, C. I.; Hong, S. W.; Kim, S.; Lee, D. K. *Biochem. Biophys. Res. Commun.* **2007**, *359*, 997–1003.